Uncovering pH at both sides of the root plasma membrane interface using noninvasive imaging.

Alexandre Martiniere, Rémy Gibrat, Herve Sentenac, Xavier Dumont, Isabelle Gaillard, Nadine Paris

Uncovering pH at both sides of the root plasma membrane interface using noninvasive imaging

Alexandre Martinière[a], Rémy Gibrat[a], Hervé Sentenac[a], Xavier Dumont[a], Isabelle Gaillard[a], and Nadine Paris[a,1]

[a]Biochimie et Physiologie Moléculaire des Plantes, Université de Montpellier, Centre National de Recherche Scientifique, L'Institut National de la Recherche Agronomique, Montpellier SupAgro, Université de Montpellier, Montpellier, France

Deborah J. Delmer, Emeritus University of California, Davis, CA, and approved April 16, 2018 (received for review December 15, 2017)

Building a proton gradient across a biological membrane and between different tissues is a matter of great importance for plant development and nutrition. To gain a better understanding of proton distribution in the plant root apoplast as well as across the plasma membrane, we generated *Arabidopsis* plants expressing stable membrane-anchored ratiometric fluorescent sensors based on pHluorin. These sensors enabled noninvasive pH-specific measurements in mature root cells from the medium–epidermis interface up to the inner cell layers that lie beyond the Casparian strip. The membrane-associated apoplastic pH was much more alkaline than the overall apoplastic space pH. Proton concentration associated with the plasma membrane was very stable, even when the growth medium pH was altered. This is in apparent contradiction with the direct connection between root intercellular space and the external medium. The plasma membrane-associated pH in the stele was the most preserved and displayed the lowest apoplastic pH (6.0 to 6.1) and the highest transmembrane delta pH (1.5 to 2.2). Both pH values also correlated well with optimal activities of channels and transporters involved in ion uptake and redistribution from the root to the aerial part. In growth medium where ionic content is minimized, the root plasma membrane-associated pH was more affected by environmental proton changes, especially for the most external cell layers. Calcium concentration appears to play a major role in apoplastic pH under these restrictive conditions, supporting a role for the cell wall in pH homeostasis of the unstirred surface layer of plasma membrane in mature roots.

pH | ratiometric sensor | root | plasma membrane

It is important for the cells of multicellular organisms to bathe in a protective interstitial environment that maintains optimal conditions for their functioning, with the potential to adapt to unfavorable external environments. In many cases, such as mammalian body fluid or insect hemolymph, the physicochemical properties of this interstitial liquid are tightly controlled by the organism (1–3). In the case of plants, a paradoxical situation exists at the level of the roots. This organ, dedicated to water and nutrient uptake, has its intercellular space (the apoplast) in direct contact with the soil. This has been demonstrated for numerous species, including the model plant *Arabidopsis*, by supplying small fluorescent dyes to the growth media, which easily penetrate the space between root cells (4, 5). From the soil, water and ions move radially through the root via an apoplastic flow, up to the cell layer known as the endodermis (6, 7). At this deep root tissue level, a polarized deposit of lignin and suberin within the apoplast forms the Casparian strip, a hydrophobic structure that prevents further diffusion toward internal cell layers. For this reason, the endodermis has been modeled as the "inner skin" of the root tissue, forcing minerals and water to enter into cells so that they can reach the internal vascular system connected to the aerial parts of the plant (8). Nevertheless, the apoplastic space of the two external cell layers, the epidermis and cortex, is not isolated from the soil and directly faces potentially unsuitable environments. This raises several questions: Are these cell layers able to regulate the physicochemical properties of their interstitial environment, and can they adjust to challenging soil compositions?

One of the physiological parameters tightly regulated in the interstitial fluid is pH. For plants, pH regulation is crucial for mineral nutrition, since it participates in the plasma membrane (PM) proton-motive force (PMF), along with the transmembrane pH gradient (PM delta pH) and an electrical component. The PMF is formed by the activity of a P-type H^+-ATPase and provides the driving force for the uptake of minerals by transporters (symporters and antiporters) and channels (9). While the electrical component of the PMF can be studied by electrophysiological approaches, it is more difficult to measure the PM delta pH in vivo. It is known that plant cells build a proton gradient across the PM, in which the apoplast is more acidic than the cytoplasm. Whereas the cytoplasmic pH is considered to be around 7.5, the pH of the apoplast can vary greatly, depending on the plant species and the measuring method. In the case of *Arabidopsis* root cells, the apoplastic pH can range from 5 to 7 (10–16). The plant apoplastic space includes the cell wall, which consists of cellulose, hemicellulose, pectins, and proteins. Due to the cation exchange properties of their negatively charged residues, pectins are thought to confer a buffering capacity to the plant cell wall, in the range of the soil pH (17). Previous studies that used a modeling approach (and were later confirmed) suggest that the pH of the cell wall could be 2 pH units more acidic than the apoplastic liquid, depending on the ionic condition of the medium (18, 19). This finding reflects the potential pH heterogeneity of the apoplast and might explain the large range in documented pH values.

In the soil, pH can vary drastically from one area to another due to nitrogen fertilizer, manure decomposition, and even acidic rain (20, 21). As a consequence, roots that face changes in soil pH must adapt themselves to these modifications.

Significance

The pH on both sides of the plant plasma membrane was accurately measured in vivo using ratiometric fluorescent sensors. This enabled noninvasive access to membrane-associated pH and transmembrane delta pH values from the surface of the root up to the deepest cell layers beyond the Casparian strip barrier. We demonstrate that despite direct contact with the soil, the apoplastic pH close to the plasma membrane was maintained at values ranging from 6.0 to 6.4 in mature root cells, whereas the overall pH in the apoplastic space is far more acidic. Furthermore, we found that the cell wall plays a role in proton homeostasis in mature root.

Author contributions: A.M., R.G., H.S., and N.P. designed research; A.M., X.D., and N.P. performed research; A.M., R.G., H.S., I.G., and N.P. analyzed data; X.D. and I.G. contributed new reagents/analytic tools; and A.M. and N.P. wrote the paper.

The authors declare no conflict of interest.

This article is a PNAS Direct Submission.

[1]To whom correspondence should be addressed. Email: nadine.paris@supagro.fr.

This article contains supporting information online at www.pnas.org/lookup/suppl/doi:10.1073/pnas.1721769115/-/DCSupplemental.

Published online June 4, 2018.

Here, to better understand proton distribution in the plant root apoplast as well as across the PM, we quantified pH on both sides of the PM using fluorescent membrane-anchored ratiometric sensors. Noninvasive pH measurements revealed differences between the epidermis and the stele in mature roots for membrane-associated pH as well as for PM delta pH. Interestingly, the root apoplastic pH remains stable even when the pH of the bathing medium is changed. The pH values found close to the PM were more alkaline than in the overall apoplastic space, which correlates well with optimal activities of channels and transporters involved in ion uptake. Lastly, our results suggest a role of the cell wall in membrane-associated pH homeostasis.

Results

Noninvasive pH Sensors Are Anchored to the PM. To investigate proton homeostasis in intact roots, we utilized ratiometric pHluorin. This is the best-described genetically encoded pH sensor with little sensitivity to other parameters such as redox status, potassium, sodium, and calcium ions (15, 22, 23). To record pH values close to the PM, we fused pHluorin to a transmembrane domain such that the fusion protein would be anchored in the PM (24) with the pH-sensing moiety facing the apoplast. As represented in Fig. 1*A*, this apoplastic membrane pH sensor, PM-Apo, has its fluorochrome positioned a few nanometers away from the PM, which is nearly 1,000 times closer to the cell surface than what can be achieved using classical pH electrodes. When transiently expressed in tobacco leaf epidermis, PM-Apo fluorescence was evenly distributed at the cell periphery, as expected for PM labeling (Fig. 1*B*). This is in contrast to the labeling pattern obtained with Apo, a secreted soluble pHluorin that can diffuse away from the membrane in the apoplast (Fig. 1*A*). As shown in Fig. 1*C*, Apo fluorescence labeling was scarce, weak, and restricted to occasional "pockets" that are likely due to acidic quenching of the pHluorin in most of the apoplast (Fig. S1*A*).

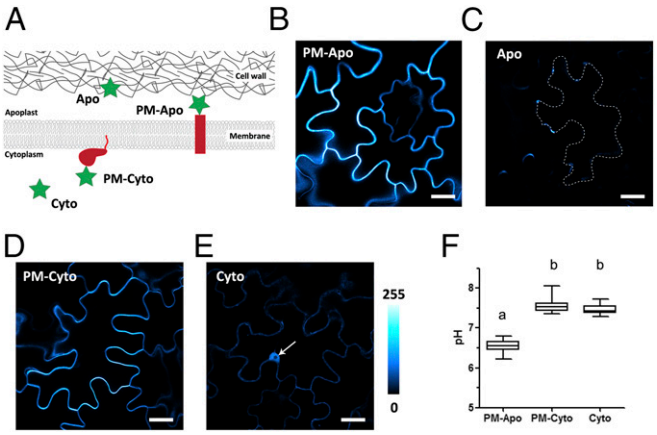

Fig. 1. Transient expression of apoplastic and cytoplasmic pH sensors in tobacco leaf epidermal cells. (*A*) Schematic representation of the pH sensors used in this study: PM-Apo and PM-Cyto are anchored at the PM on either side of the two membrane faces. PM-Apo is anchored by a 26-amino acid transmembrane domain, whereas PM-Cyto is anchored due to the C-terminal region of Ras, which includes a farnesylation signal. Cyto is a free soluble pHluorin expressed in the cytosol, and Apo is a soluble pHluorin secreted by default. (*B*–*E*) Confocal images of tobacco epidermal cells expressing PM-Apo (*B*), Apo (*C*), PM-Cyto (*D*), and Cyto (*E*) constructs (arrow in *E* indicates nucleus). The four images were taken using the same confocal settings. False color is indicative of fluorescence intensity. (Scale bars: 20 μm.) Apo barely labels the apoplast (see dotted line in *C*), whereas PM-Apo (shown in *B*) is evenly distributed at the cell periphery. (*F*) Comparison of apoplastic or cytoplasmic pH measurements obtained with free or membrane-anchored sensors. $n > 18$; ANOVA followed by Tukey's test; $P < 0.05$ between a and b groups.

To quantify the PM delta pH, we also designed a sensor anchored in the inner face of the PM. For this, we fused pHluorin to the farnesylation sequence of Ras (25) and named it PM-Cyto (Fig. 1*A*). As shown in Fig. 1*D*, the labeling of tobacco epidermal cells expressing PM-Cyto is restricted to the cell periphery (Fig. 1*D*) and does not include the nucleus, in contrast to Cyto labeling (Fig. 1*E*) obtained with a cytoplasmic soluble pHluorin (Fig. 1*A*). The membrane localization of PM-Apo and PM-Cyto was further assayed by the plasmolysis experiment and microsomal fractionation (Fig. S1 *B* and *C*, respectively).

Next, the fluorescence ratio was assessed from tobacco epidermal cells expressing the different sensors, and the corresponding pH values were calculated using an in situ calibration with a recombinant pHluorin (Fig. S2). An average pH value of 6.5 was detected at the outer face of the PM in the tobacco epidermis (PM-Apo, Fig. 1*F*). The different labeling patterns obtained for the two apoplastic sensors (Fig. 1 *B* and *C*) and the acidic quenching of Apo (Fig. S1*A*) suggest that the extracellular environment has a heterogenous pH. In contrast, the PM–cytosol interface and the entire cytosol (PM-Cyto and Cyto, respectively; Fig. 1*F*) both displayed a pH of 7.5. Due to the pH value obtained at the outer face of the PM, two altered versions of PM-Apo were generated with modified linkers between the sequences of the transmembrane domain and the pHluorin—PM-Apo(bis) and PM-Apo(ter)—and their PM localization was further assayed by plasmolysis (Fig. S3*A*). The three PM-Apo sensors are predicted to expose the pHluorin at various distances from the PM (Fig. S3*B*). The pH values obtained in tobacco epidermal cells with the two additional membrane-anchored sensors were slightly but significantly more alkaline than PM-Apo (Fig. S3*C*, *P* value <0.05). Interestingly, in tobacco protoplasts, this difference is abolished (Fig. S3*D*). Altogether, this suggests that pH measurement in close vicinity to PM is little impacted by the linker structure but is affected by the cell wall. Lastly, the membrane orientation of the PM-associated pH sensors was assayed by two different approaches (Fig. S4). A proteinase K digest on living cells (26) was performed on tobacco protoplasts, which led to a clear decrease of PM-Apo fluorescence as compared to PM-Cyto (Fig. S4*A*). Similarly, a proteinase K digest on *Arabidopsis* microsomes led to opposite responses of two PM sensors (Fig. S4*B*), a result that is also in accordance with pHluorin being exposed outside of the cell for PM-Apo and protected from digestion in PM-Cyto configuration. Altogether, our results with membrane-anchored sensors revealed an apoplastic pH of 6.5 to 6.7 close to the PM, and a cytoplasmic pH of 7.5 in tobacco epidermal cells.

***Arabidopsis* Roots Present Radial Variation in pH at the Apoplastic Interface of the PM, Leading to a Maximal PM Delta pH in Stele Cells.** Transgenic *Arabidopsis* plants expressing one of the two pHluorin-based sensors anchored on either side of the PM (PM-Apo and PM-Cyto) were generated. These plants did not present any visible growth phenotype compared with wild-type plants (Fig. S5*A*) and were able to acidify their growth media (Fig. S5*B* and ref. 27). A detailed analysis of pH by confocal macroscope on intact *Arabidopsis* plantlets revealed two acidic root zones (Fig. S6*A*), in agreement with previous reports using other approaches (11, 28–30). Next, the ability of PM-associated sensors to detect transmembrane transport mechanisms in mature root was confirmed using orthovanadate, an inhibitor of P-ATPase (Fig. S6*B*), and nigericin, a proton ionophore (Fig. S6*C*). In contrast, applying PM depolarization treatments either by increasing potassium concentration in the media or by adding the K^+ ionophore valinomycin (31) did not affect PM-Apo pH (Fig. S7 *B* or *C*, respectively). To confirm the impact of the different treatment on membrane potential, we used the voltage-sensitive fluorescent dye bis-(1,3-dibutylbarbituric acid) trimethine oxonol [DiBAC4(3)] which exhibits an enhanced fluorescence when bound to depolarized membranes (refs. 32 and 33 and Fig. S7*A*). This

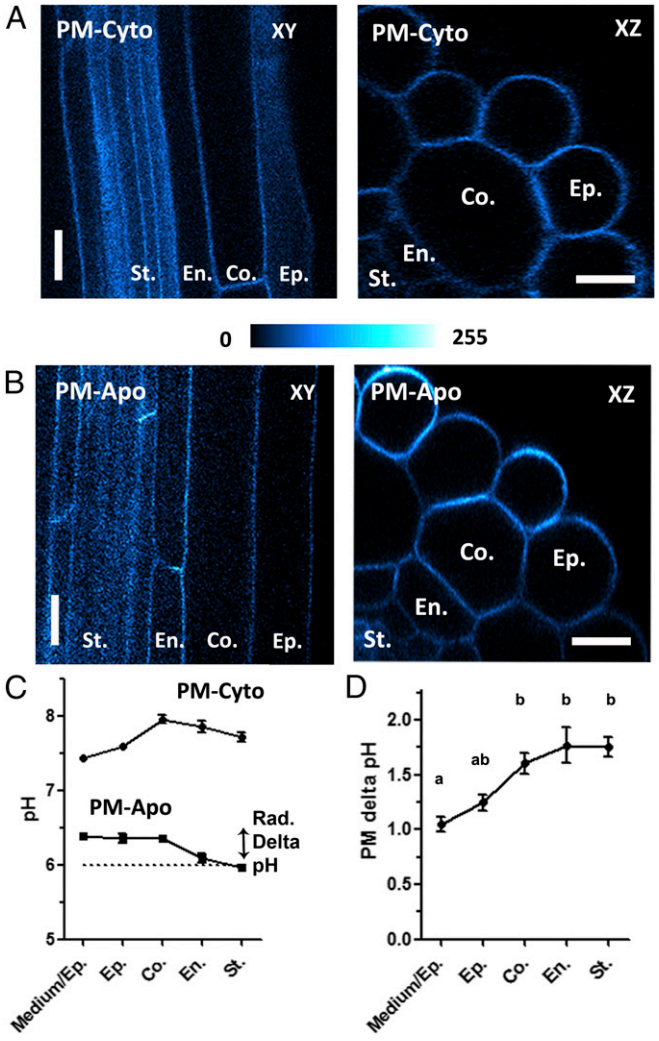

Fig. 2. Stable expression of membrane-anchored pH sensors in mature *Arabidopsis* roots. (*A* and *B*) Representative optical sectioning obtained by confocal microscopy of the mature roots of 6-d-old plantlets expressing PM-Cyto (*A*) or PM-Apo (*B*). XY: median longitudinal confocal section of 1 Airy; XZ: radial section obtained by 3D projection of 50-μm z stacks. False color is indicative of fluorescence intensity. (Scale bars: 10 μm.) (*C*) Cell type-specific measurements of pH along the radial axis of the mature root in MS/2 medium (pH 6, dotted line) and expressing either PM-Apo or PM-Cyto. Radial (Rad.) delta pH is the difference in $pH_{apo\text{-}PM}$ between the root surface and the stele. (*D*) The cell layer-specific PM delta pH for each cell layer (determined as the difference between the PM-Cyto and PM-Apo probed pH values). $n > 29$; mean ± SEM; ANOVA followed by Tukey's test by cell layers; $P < 0.05$ between a and b groups. Co., cortex; En., endodermis; Ep., epidermis; Medium/Ep., the PM at the interface between the media and the root epidermis; St., stele.

suggests that fluorescence from PM-Apo was not affected by the electron motive force at the PM.

Subsequently, we analyzed PM-associated pH on the portion of roots with expanded hairs located roughly 2 cm from the apex and a fully differentiated Casparian strip, as confirmed by staining with propidium iodide (Fig. S8*A*, purple). The fluorescent signals of the PM-Cyto (Fig. 2*A*) and PM-Apo (Fig. 2*B*) sensors were limited to the periphery of the root cells and were detected all the way down to the stele using confocal microscopy on intact plantlets, as revealed in xy optical sections and xz projections (Fig. 2 *A* and *B*). In comparison, no signal was detected from nontransformed plants (Fig. S9*A*).

Using xz projections of transformed mature roots, cell layer-specific fluorescence data were collected at the medium–epidermis interface or between two isotypic cells (Fig. S8*B*), and the pH was calculated using in situ calibration curves (Fig. S2*B*). As shown in Fig. 2*C* (*Bottom* curve), the apoplastic pH observed close to the PM (i.e., $pH_{apo\text{-}PM}$) was stable at pH 6.4, from the medium–epidermis interface up to the cortex. Several approaches were performed to investigate the apoplastic pH further away from the PM, including the transformation of *Arabidopsis* plants with the Apo construct. Unfortunately, as previously described for the pH sensor apopHusion (16), most of the fluorescence signal was retained in the endoplasmic reticulum (ER), especially in the mature part of the root (Fig. S10*A*, arrows), making accurate pH measurements extremely difficult. We then used the fluorescent probe 8-hydroxypyrene-1,3,6-trisulfonic acid trisodium salt (HPTS) (Fig. S10*C*) and estimated the overall apoplastic pH as 5.7 (Fig. S10*H*). This is likely an overestimation of the apoplastic space pH, since the 450-nm excitation peak of HPTS was missing at pH 5. Lastly, the pH dye Oregon Green dextran was used as previously described (34), except for application of an additional gentle vacuum (Fig. S10*B*); this permitted us to estimate the overall apoplastic pH to be close to 4 (Fig. S10*H*). Altogether, these results indicate that in mature roots, the apoplastic pH close to the PM is more alkaline than the average pH of the apoplastic space.

Deeper in the root tissue (e.g., the endodermis and the stele), $pH_{apo\text{-}PM}$ was significantly more acidic than in more peripheral cell layers (Fig. 2*C* and Fig. S11). This difference in $pH_{apo\text{-}PM}$ along the radial axis in the mature root was named radial delta $pH_{apo\text{-}PM}$ (Fig. 2*C*). This positive radial delta pH value is in opposition to a simple model of proton diffusion between the medium and the entire root apoplastic space and shows a tight regulation of PM-associated pH in the mature root (including the outermost cell layer).

Similarly, cell layer-specific cytoplasmic pH values were measured from roots expressing PM-Cyto (i.e., pH_{cyto}) (Fig. 2*C*, *Top* curve). Importantly, the two sets of collected pH values allowed us to calculate the transmembrane proton gradient (PM delta pH = $pH_{cyto} - pH_{apo\text{-}PM}$) for each cell layer in a noninvasive manner. This PM delta pH measurement is directly linked to the PMF of the PM, which increases from the medium–epidermis interface to the internal cell layers where it reaches an optimum of 1.7 pH units in the endodermis and the stele (Fig. 2*D*).

The Radial Variation of $pH_{apo\text{-}PM}$ Is Highly Robust in Mature Roots. The root apoplastic space is in direct contact with the bulk media, shown by diffusion of propidium iodide in the root (Fig. S8*A*). As a consequence, the apoplastic liquid should be highly sensitive to any fluctuation in proton concentration in the medium. The impact of modifying the pH of half-strength Murashige and Skoog (MS/2) medium on steady-state apoplastic PM-associated pH was therefore investigated in mature roots and was found to have no effect at all on either the endodermis or the stele $pH_{apo\text{-}PM}$ (Fig. 3*A*). Only small changes were detected in the outer cell layers up to the cortex, where $pH_{apo\text{-}PM}$ was observed to increase even when a pH value of 5 was applied, although further analysis of the data revealed no statistical difference between pH 5 and pH 6 or between pH 7 and pH 8 for the epidermis and the cortex (Fig. 3*A*). As shown in Fig. 3*B*, the measured $pH_{apo\text{-}PM}$ was mostly preserved, even at the interface between the root and the medium, as changing the bulk proton concentration by up to 3 orders of magnitude resulted in only a variation of 0.7 pH units at most. No effect on the apoplastic pH was observed in the stele (Fig. 3*B*). We observed that the radial delta $pH_{apo\text{-}PM}$ was not abolished by acidifying the external medium, and it was even amplified in more alkaline conditions (Fig. 3*C*). A similar mild effect was observed with stronger buffering capacities of the medium (Fig. S12 *A* and *B*).

These results demonstrate that the pH of the apoplast in close proximity to the PM is very stable in MS/2 medium and that it is mostly unaffected by external conditions. This indicates that a radial PM-associated apoplastic delta pH value of at least 0.4 pH

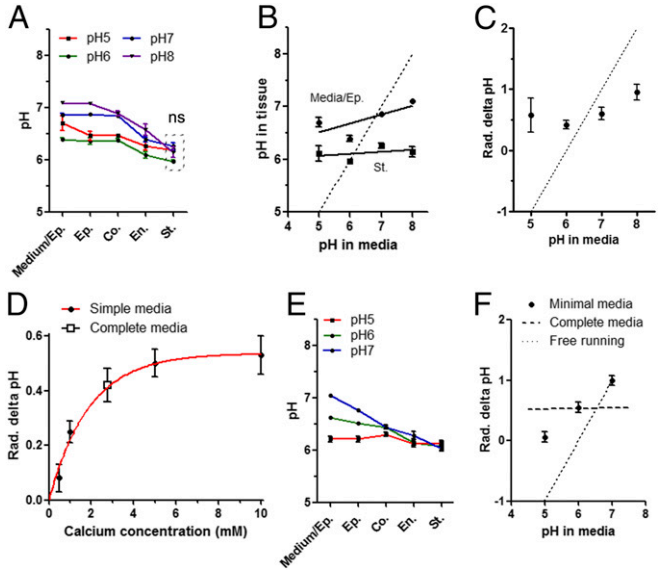

Fig. 3. Apoplastic pH homeostasis close to the PM in *Arabidopsis* mature roots. *Arabidopsis* plantlets expressing PM-Apo were grown for 5 d on MS/2 medium (pH 6) and transferred for 24 h onto complete MS/2 medium at different pH levels (*A*–*C*) or onto minimal KCl medium (*D*–*F*) before pH measurement in the mature part of the root. (*A*) Cell layer-specific $pH_{apo\text{-}PM}$ at various pH levels. (*B*) $pH_{apo\text{-}PM}$ at the medium–epidermis interface (Media/Ep.) and the stele as a function of the pH in the medium. (*C*) Radial (Rad.) apoplastic delta $pH_{apo\text{-}PM}$ as a function of the pH in the medium. (*D*) Root radial delta $pH_{apo\text{-}PM}$ at different calcium concentrations in minimal medium containing 10 mM KCl (pH 6; closed circles) or in complete MS/2 medium (containing 2 mM Ca^{2+} and 0.75 mM Mg^{2+}, pH 6; open square). (*E*) Cell layer-specific $pH_{apo\text{-}PM}$ at different pH levels. (*F*) Root radial delta $pH_{apo\text{-}PM}$ as a function of the pH. Dotted line in *B*, *C*, and *F* represents what would be expected for a free-running system, in which pH in the stele is equilibrated with the pH of the medium. $n > 16$; mean ± SEM; ANOVA followed by Tukey's test by cell layers; $P < 0.05$; ns indicates non-significant difference for measures included in dashed line box. Co., cortex; En., endodermis; Ep., epidermis; Medium/Ep., the PM at the interface between the media and the root epidermis; St., stele.

units was preserved throughout the root tissue, with the pH in the stele strictly maintained at pH 6.1 in MS/2 medium.

The Calcium and Proton Variation in Minimal Medium Influences the PM-Associated pH Observed in Mature Roots. To further investigate the effect of ions on root pH, we replaced the complete medium with minimal ionic medium composed of 5 mM KCl to which we added various Ca^{2+} concentrations below and above that of MS/2 medium. At equilibrium, the calcium concentration was observed to have a major effect on the radial delta $pH_{apo\text{-}PM}$, which appears to follow a saturating mechanism, with an optimum of 0.5 pH units for 5 mM calcium and above (Fig. 3*D*). The best fit was found using an exponential relation for radial delta $pH_{apo\text{-}PM}$ and calcium concentration ($R^2 = 0.97$, $K_d = 1.9$ mM). Moreover, the value previously obtained under MS/2 conditions (2 mM Ca^{2+} and 0.75 mM Mg^{2+}) fits perfectly with this curve (Fig. 3*D*, square).

For the following experiments, we chose a concentration of 10 mM $CaCl_2$, which provides a $CaCl_2$/KCl ratio of 2 and, under this condition, the potassium concentration associated with the cell wall is predicted to be marginal (18). Using these conditions, the $pH_{apo\text{-}PM}$ values obtained in minimal medium were compared with those previously obtained in complete medium (MS/2 medium) at the same pH level (pH 6), and no differences were detected (Fig. S12*C*). Next, $pH_{apo\text{-}PM}$ robustness was challenged with various external proton concentrations. As shown in Fig. 3*E*, the $pH_{apo\text{-}PM}$ values followed the bulk pH in the most external cell layers, but not in the endodermis or the stele. Consequently, the steady-state radial delta $pH_{apo\text{-}PM}$ increased in a linear manner together with the alkalinization of the minimal medium, which is in contrast to what was observed in complete medium (see Fig. 3*F* vs. Fig. 3*C*).

For further insight into pH regulation across the PM, we monitored proton concentration at the inner face of the PM in mature roots (Fig. S12*D*) and calculated the PM delta pH (Fig. S12*E*). At any of the three pH levels tested, the PM delta pH increased from the epidermis to the stele where it reached an optimum of 2 pH units (Fig. S12*E*). For the endodermis, we observed an alkalinization of pH_{cyto} at pH 7 (Fig. S12*D*, blue), suggesting that the plant can also compensate for environmental constraints by modulating cytoplasmic PM-associated pH by cell layer-specific mechanisms. As a result of decreasing the minimal medium pH to 5, the radial delta $pH_{apo\text{-}PM}$ is close to zero (Fig. 3*E*). This result strongly differs from those obtained in complete medium (Fig. 3*A*, red).

Altogether, these results demonstrate that K^+, Cl^-, and Ca^{2+} are less efficient at maintaining proton homeostasis in the external cell layer than the complex set of ions provided by complete medium (MS/2). It also demonstrates that Ca^{2+} has a significant impact on the radial delta $pH_{apo\text{-}PM}$ in mature roots equilibrated with a minimal KCl medium.

In Minimal Medium, the Anion Species Has Little Impact on the PM-Associated pH Observed in Mature Roots. After determining that minimal medium conditions conferred less root pH robustness to environmental constraints than complete medium, we next tested the impact of anion species. We chose two major anions that are expected to affect root pH: SO_4^{2-}, which is less absorbed than Cl^-; and NO_3^-, which is more absorbed than Cl^- (35). Moreover, both SO_4^{2-} and NO_3^- require proton cotransport for their uptake: Sulfate is believed to consume three protons and nitrate is believed to consume two protons (36, 37). The pH on either side of the PM was measured in mature roots of plants expressing PM-Apo and PM-Cyto, after equilibration in either KNO_3/$CaCl_2$ or K_2SO_4/$CaCl_2$ conditions at pH 5, 6, or 7 (Fig. S13 *A*, *B*, *D*, and *E*). Changing the nature of the anion had no effect on the radial delta $pH_{apo\text{-}PM}$ (Fig. S13*C*). The calculated PM delta pH of each cell layer for the NO_3^- (Fig. S13*F*) and SO_4^{2-} (Fig. S13*G*) conditions was unexpectedly stable in comparison with Cl^- (Fig. S12*E*). These results could be explained by the fact that a majority of the anion channels/transporters characterized so far transport both Cl^- and NO_3^- (38). Altogether, our results suggest that PM-associated pH is barely affected by the nature of the anion, suggesting the presence of potential compensatory mechanisms.

Discussion

Here, we established that membrane-anchored ratiometric pH sensors allow the noninvasive measurement of PM delta pH in various cell types of living *Arabidopsis* roots, including in the central cylinder. Our results demonstrate that the apoplastic pH in the unstirred surface layer of the PM is both strictly controlled and far from behaving as a free-running system, as initially expected from the continuity between the cell apoplast and the medium up to the endodermis. Lastly, the cell wall appears to have a regulatory role of the apoplastic pH.

Homeostatic Regulation of PM-Associated Apoplastic pH in *Arabidopsis* Roots. *Arabidopsis* displays a conserved gradient of $pH_{apo\text{-}PM}$ in the mature root, wherein the stele is on average 0.4 pH units more acidic than the surface. When looking more closely at the distribution of pH at the level of each cell layer, it is clear that the proton concentration in the apoplastic interface of the PM does not gradually vary along a radial axis. Instead, the root is divided into two zones: an "alkaline" zone including the surface of the root, the epidermis, and the cortex; and an "acidic" zone containing the endodermis and the stele (Fig. S11). Because we performed our measurements in a fully developed part of the root

with a mature Casparian strip, the pH "break" in the root apoplast can be observed to coincide with this structure in the endodermis. The Casparian strip is the main barrier for apoplastic diffusion of solutes and plays a central role in current models of plant nutrient uptake by roots. Indeed, when this barrier is deficient, as in the *schengen3* mutant, a major defect in maintaining sufficient levels of macronutrients such as potassium can be observed (39). Therefore, it is possible that the Casparian strip contributes to the control of PM-associated apoplastic pH in plants.

Surprisingly, even the peripheral cell layers that are in direct contact with the medium appeared to "resist" against pH variation within the medium. These observations suggest the potential existence of strong compensatory mechanisms that appear more efficient in complete medium (Fig. S13*H*). The two major P-type ATPases in *Arabidopsis* roots, AHA1 and AHA2, are known to participate in media acidification and are necessary for plant growth in alkaline conditions (40–43). Interestingly, AHA2 activity is regulated by PKS5 kinase, which is in turn regulated by apoplastic pH (44). One in vitro study has elegantly demonstrated that a PM delta pH value higher than 2 acts directly on AHA2 activity via allosteric regulation (45). This illustrates the tight link between apoplastic pH and the activity of P-type ATPase, and might explain why in our in vivo measurement the PM delta pH saturates at 2 pH units. We could not exclude that the channel and transporter, in addition to the P-type ATPase regulation, participate in pH homeostasis. To test this hypothesis, we modified the anion species, but this resulted in little effect, suggesting that chloride, nitrate, or sulfate alone cannot restore the apoplastic pH robustness observed in complete medium. We also examined the role of calcium and determined that it acts on the radial difference of $pH_{PM\text{-}Apo}$ between the two sides of the endodermal cell layer. Cell wall appears to be the biggest pool of calcium ion in plant tissues (46), with a several-millimolar concentration in horse bean and yellow lupine root (18) and 6 mM in soybean roots (47). Calcium is known as a crucial regulator of growth and development in plants (48). Modification of cell wall extensibility and cell growth are essential for the processes leading to shape plants. These modifications in stiffness are in part attributed to Ca^{2+} interaction with pectate, more precisely to the free carboxyl groups that are present in pectin, a major component of primary cell wall (49, 50). Thus, calcium depletion could free up the cell wall acidic group and modify the cell wall cation exchange capacity or buffering effect of pectin. Interestingly, radial heterogeneity of calcium association with the cell wall has been described in *Brachypodium* roots (51).

The strong homeostatic behavior of root cell apoplastic pH at the membrane interface is paralleled by the conservation of the delta pH formed through the PM. In MS/2 medium, we found that the PM delta pH gradually increases from the outer cell layer to the stele (from 1 to almost 2 pH units). Numerous transport and channel activities are regulated by PM delta pH. Nitrate transporter 1/peptide transporter family (NPF) proteins like NPF6.3 or NPF2.7 that are expressed in root outer layers are functional in heterologous systems when the PM delta pH is close to 1 pH unit (31, 52, 53). By contrast, NPF7.2 or NFP4.6, which are found in the root inner tissue, require a higher PM delta pH (close to 2 pH units) to generate a substantial transport activity (54–56). The expression pattern of these NPF genes is in agreement with our in vivo observed PM delta pH, in which the outer layers of the root have smaller PM delta pH values than those in the stele. In the case of potassium channels, their regulation by pH at the PM is also well documented (57). For example, the stelar K^+ outward rectifier channel SKOR that is involved in potassium release into the xylem sap toward the shoot (58) is modulated both by inner and outer pH levels at the PM (59). Interestingly, with pH 7.7 in the cytosol and pH 6 in the apoplasm in the stele (Fig. 2*C*), SKOR should only be at 50% of its optimal activity, suggesting a full potential to regulate potassium secretion into xylem via pH. The inwardly rectifying potassium channel AKT1 (60) is functional in Sf9 with a PM delta pH of 1 unit (61) and is expressed in the root epidermis and cortex (62). It is therefore functional in the most external cell layers where PM delta pH values are the lowest, which agrees with the attributed function of AKT1 as the main channel for potassium uptake from the soil by roots in high potassium concentration (63).

Apoplastic pH Close to the PM Is More Alkaline than in the Overall Apoplastic Space. To date, apoplastic pH in plants has primarily been investigated using either electrodes or fluorescent ratiometric components that diffuse into the apoplast. Although these methods allow the rapid measurement of pH, they are limited by the accessibility of the internal cell layers. Even small fluorescent molecules cannot pass through the Casparian strip, leaving the central cell layers inaccessible. This limitation was potentially surmounted by generating genetically encoded pH sensors that can accumulate in the apoplast via secretion. However, such sensors can diffuse out of the tissue and can also accumulate in the ER, which complicates apoplastic pH measurements, especially in turgescent cells such as mature root cells (15, 16). We resolved these problems by anchoring pHluorin to the PM with a transmembrane domain and executing repetitive imaging of all root cell layers up to the central cylinder in *Arabidopsis*. The $pH_{apo\text{-}PM}$ values that were obtained with our PM-anchored sensor in mature roots grown in rich medium ranged from 6.0 to 6.3, depending on the cell type. This range is close to the value found using a secreted At-pHluorin (pH 6.3) in the lateral roots of 1- to 4-wk-old *Arabidopsis* plants (15, 16). This is in contrast to the more acidic cell wall measurements obtained from roots perfused with small fluorescent probes, with pH levels detected between 4 and 5.7 in mature roots (this work) and ranging from pH 4.2 to 5.3 in *Arabidopsis* root cells, from pH 5 to 6 in maize, or close to pH 5.2 in lupine tap roots (64, 65). Altogether, these results indicate the existence of a complex apoplastic environment, with a potential unstirred layer in the vicinity of the PM where pH is more alkaline than in the entire apoplastic liquid and with an acidic Donnan space associated with the cell wall. This raises the question of how such a gradient can be maintained, since the source of apoplast acidity should come from the activity of P-type ATPase localized at the PM (40). One possible explanation for this paradoxical situation is that the net proton extrusion recorded in Fig. S6 *B* and *C* is not coming from the root zone observed in our experiment. Indeed, it is generally accepted that the *Arabidopsis* root tip is acidic and therefore could alone be responsible for the medium acidification. If true, this would suggest that in fully differentiated tissue of *Arabidopsis*, a net influx of protons is taking place (66). It would be of great interest to further study this complex apoplastic environment, including in regions more than a few nanometers from the lipid bilayer, although this would require sensors that are not quenched below pH 5. The ability of these PM-associated sensors to monitor pH variation independent of membrane potential changes and within minutes after treatment also provides a great tool for the future study of pH on either side of the PM in potentially all cell types (including those not directly accessible), including using caged protons (67).

Materials and Methods

A full discussion of the materials and methods can be found in *SI Materials and Methods*.

Arabidopsis plants expressing PM-Apo and PM-Cyto were grown for 5 to 6 d in MS/2 medium supplemented with 2.5 mM MES-KOH (pH 6), 1% sucrose, and 0.8% agar type E. Before microscopy observations, plantlets were transferred to treatment plates for 24 h. Samples in the mature part of root were illuminated sequentially at 476 and 496 nm with a confocal microscope and a z stack was generated where indicated. Fluorescence ratios were obtained and were converted into pH values using a calibration curve generated in situ with a recombinant pHluorin produced in *Escherichia coli* (15, 23, 68, 69).

ACKNOWLEDGMENTS. We thank Yvon Jaillais for the 8K Farn construct, Gabriel Krouk for his help on statistical analysis, and the Montpellier Ressources Imagerie and the Histocytology and Plant Cell Imaging Platform for providing the microscope facility. This work was funded by the Rhizopolis project from the Agropolis Foundation and the SweetKaliGrape project from the French National Research Agency.

1. Beyenbach KW (2016) The plasticity of extracellular fluid homeostasis in insects. *J Exp Biol* 219:2596–2607.
2. Cannon WB (1929) Organization for physiological homeostasis. *Physiol Rev* 9:399–431.
3. Takei Y (2000) Comparative physiology of body fluid regulation in vertebrates with special reference to thirst regulation. *Jpn J Physiol* 50:171–186.
4. Carpita N, Sabularse D, Montezinos D, Delmer DP (1979) Determination of the pore size of cell walls of living plant cells. *Science* 205:1144–1147.
5. Kramer EM, Frazer NL, Baskin TI (2007) Measurement of diffusion within the cell wall in living roots of *Arabidopsis thaliana*. *J Exp Bot* 58:3005–3015.
6. Barberon M, Geldner N (2014) Radial transport of nutrients: The plant root as a polarized epithelium. *Plant Physiol* 166:528–537.
7. Nawrath C, et al. (2013) Apoplastic diffusion barriers in *Arabidopsis*. *Arabidopsis Book* 11:e0167.
8. Alassimone J, Roppolo D, Geldner N, Vermeer JEM (2012) The endodermis–Development and differentiation of the plant's inner skin. *Protoplasma* 249:433–443.
9. Nelson N (1994) Energizing porters by proton-motive force. *J Exp Biol* 196:7–13.
10. Barbez E, Dünser K, Gaidora A, Lendl T, Busch W (2017) Auxin steers root cell expansion via apoplastic pH regulation in *Arabidopsis thaliana*. *Proc Natl Acad Sci USA* 114:E4884–E4893.
11. Staal M, et al. (2011) Apoplastic alkalinization is instrumental for the inhibition of cell elongation in the *Arabidopsis* root by the ethylene precursor 1-aminocyclopropane-1-carboxylic acid. *Plant Physiol* 155:2049–2055.
12. Bibikova TN, Jacob T, Dahse I, Gilroy S (1998) Localized changes in apoplastic and cytoplasmic pH are associated with root hair development in *Arabidopsis thaliana*. *Development* 125:2925–2934.
13. Monshausen GB, Bibikova TN, Weisenseel MH, Gilroy S (2009) Ca2+ regulates reactive oxygen species production and pH during mechanosensing in *Arabidopsis* roots. *Plant Cell* 21:2341–2356.
14. Monshausen GB, Miller ND, Murphy AS, Gilroy S (2011) Dynamics of auxin-dependent Ca2+ and pH signaling in root growth revealed by integrating high-resolution imaging with automated computer vision-based analysis. *Plant J* 65:309–318.
15. Gao D, Knight MR, Trewavas AJ, Sattelmacher B, Plieth C (2004) Self-reporting *Arabidopsis* expressing pH and [Ca2+] indicators unveil ion dynamics in the cytoplasm and in the apoplast under abiotic stress. *Plant Physiol* 134:898–908.
16. Gjetting KS, Ytting CK, Schulz A, Fuglsang AT (2012) Live imaging of intra- and extracellular pH in plants using pHusion, a novel genetically encoded biosensor. *J Exp Bot* 63:3207–3218.
17. Meychik NR, Yermakov IP (2001) Ion exchange properties of plant root cell walls. *Plant Soil* 234:181–193.
18. Sentenac H, Grignon C (1981) A model for predicting ionic equilibrium concentrations in cell walls. *Plant Physiol* 68:415–419.
19. Sentenac H, Grignon C (1987) Effect of H excretion on the surface pH of corn root cells evaluated by using weak acid influx as a pH probe. *Plant Physiol* 84:1367–1372.
20. López-Arredondo DL, Leyva-González MA, Alatorre-Cobos F, Herrera-Estrella L (2013) Biotechnology of nutrient uptake and assimilation in plants. *Int J Dev Biol* 57:595–610.
21. Singh A, Agrawal M (2008) Acid rain and its ecological consequences. *J Environ Biol* 29:15–24.
22. Miesenböck G, De Angelis DA, Rothman JE (1998) Visualizing secretion and synaptic transmission with pH-sensitive green fluorescent proteins. *Nature* 394:192–195.
23. Martinière A, et al. (2013) In vivo intracellular pH measurements in tobacco and *Arabidopsis* reveal an unexpected pH gradient in the endomembrane system. *Plant Cell* 25:4028–4043.
24. Brandizzi F, et al. (2002) The destination for single-pass membrane proteins is influenced markedly by the length of the hydrophobic domain. *Plant Cell* 14:1077–1092.
25. Simon MLA, et al. (2016) A PtdIns(4)P-driven electrostatic field controls cell membrane identity and signalling in plants. *Nat Plants* 2:16089.
26. Lorenz H, Hailey DW, Wunder C, Lippincott-Schwartz J (2006) The fluorescence protease protection (FPP) assay to determine protein localization and membrane topology. *Nat Protoc* 1:276–279.
27. Gujas B, Alonso-Blanco C, Hardtke CS (2012) Natural *Arabidopsis* brx loss-of-function alleles confer root adaptation to acidic soil. *Curr Biol* 22:1962–1968.
28. Peters WS, Felle HH (1999) The correlation of profiles of surface pH and elongation growth in maize roots. *Plant Physiol* 121:905–912.
29. Monshausen GB, Zieschang HE, Sievers A (1996) Differential proton secretion in the apical elongation zone caused by gravistimulation is induced by a signal from the root cap. *Plant Cell Environ* 19:1408–1414.
30. Zieschang HE, Köhler K, Sievers A (1993) Changing proton concentrations at the surfaces of gravistimulated phleum roots. *Planta* 190:546–554.
31. Segonzac C, et al. (2007) Nitrate efflux at the root plasma membrane: Identification of an *Aarabidopsis* excretion transporter. *Plant Cell* 19:3760–3777.
32. Konrad KR, Hedrich R (2008) The use of voltage-sensitive dyes to monitor signal-induced changes in membrane potential-ABA triggered membrane depolarization in guard cells. *Plant J* 55:161–173.
33. Dejonghe W, et al. (2016) Mitochondrial uncouplers inhibit clathrin-mediated endocytosis largely through cytoplasmic acidification. *Nat Commun* 7:11710.
34. Geilfus C-MMS, Mühling KH (2011) Real-time imaging of leaf apoplastic pH dynamics in response to NaCl stress. *Front Plant Sci* 2:13.
35. Keltjens WG (1981) Absorption and transport of nutrient cations and anions in maize roots. *Plant Soil* 63:39–46.
36. Hawkesford MJ (2011) Sulfate transport. *The Plant Plasma Membrane*, eds Murphy A, Schulz B, Peer W, Plant Cell Monographs (Springer, Berlin), Vo. 19, pp 291–301.
37. Meharg AA, Blatt MR (1995) $NO3^-$ transport across the plasma membrane of *Arabidopsis thaliana* root hairs: Kinetic control by pH and membrane voltage. *J Membr Biol* 145:49–66.
38. Barbier-Brygoo H, et al. (2011) Anion channels/transporters in plants: From molecular bases to regulatory networks. *Annu Rev Plant Biol* 62:25–51.
39. Pfister A, et al. (2014) A receptor-like kinase mutant with absent endodermal diffusion barrier displays selective nutrient homeostasis defects. *eLife* 3:e03115.
40. Falhof J, Pedersen JT, Fuglsang AT, Palmgren M (2016) Plasma membrane H^+-ATPase regulation in the center of plant physiology. *Mol Plant* 9:323–337.
41. Haruta M, et al. (2010) Molecular characterization of mutant *Arabidopsis* plants with reduced plasma membrane proton pump activity. *J Biol Chem* 285:17918–17929.
42. Haruta M, Sussman MR (2012) The effect of a genetically reduced plasma membrane protonmotive force on vegetative growth of *Arabidopsis*. *Plant Physiol* 158:1158–1171.
43. Haruta M, Tan LX, Bushey DB, Swanson SJ, Sussman MR (2018) Environmental and genetic factors regulating localization of the plant plasma membrane H^+-ATPase. *Plant Physiol* 176:364–377.
44. Fuglsang AT, et al. (2007) Arabidopsis protein kinase PKS5 inhibits the plasma membrane H^+-ATPase by preventing interaction with 14-3-3 protein. *Plant Cell* 19: 1617–1634.
45. Veshaguri S, et al. (2016) Direct observation of proton pumping by a eukaryotic P-type ATPase. *Science* 351:1469–1473.
46. Demarty M, Morvan C, Thellier M (1984) Calcium and the cell wall. *Plant Cell Amp Environ* 7:441–448.
47. Hayatsu M, Suzuki S (2015) Electron probe X-ray microanalysis studies on the distribution change of intra- and extracellular calcium in the elongation zone of horizontally reoriented soybean roots. *Microscopy (Oxf)* 64:327–334.
48. Hepler PK (2005) Calcium: A central regulator of plant growth and development. *Plant Cell* 17:2142–2155.
49. Cosgrove DJ (2016) Catalysts of plant cell wall loosening. *F1000 Res* 5:F1000 Faculty Rev-119.
50. Hocq L, Pelloux J, Lefebvre V (2017) Connecting homogalacturonan-type pectin remodeling to acid growth. *Trends Plant Sci* 22:20–29.
51. Pacheco-Villalobos D, et al. (2016) The effects of high steady state auxin levels on root cell elongation in *Brachypodium*. *Plant Cell* 28:1009–1024.
52. Parker JL, Newstead S (2014) Molecular basis of nitrate uptake by the plant nitrate transporter NRT1.1. *Nature* 507:68–72.
53. Noguero M, Lacombe B (2016) Transporters involved in root nitrate uptake and sensing by *Arabidopsis*. *Front Plant Sci* 7:1391.
54. Li J-Y, et al. (2010) The *Arabidopsis* nitrate transporter NRT1.8 functions in nitrate removal from the xylem sap and mediates cadmium tolerance. *Plant Cell* 22: 1633–1646.
55. Huang N-C, Liu K-H, Lo H-J, Tsay Y-F (1999) Cloning and functional characterization of an *Arabidopsis* nitrate transporter gene that encodes a constitutive component of low-affinity uptake. *Plant Cell* 11:1381–1392.
56. Kanno Y, et al. (2012) Identification of an abscisic acid transporter by functional screening using the receptor complex as a sensor. *Proc Natl Acad Sci USA* 109: 9653–9658.
57. Maathuis FJM, Sanders D (1996) Mechanisms of potassium absorption by higher plant roots. *Physiol Plant* 96:158–168.
58. Gaymard F, et al. (1998) Identification and disruption of a plant shaker-like outward channel involved in K^+ release into the xylem sap. *Cell* 94:647–655.
59. Lacombe B, Pilot G, Gaymard F, Sentenac H, Thibaud J-B (2000) pH control of the plant outwardly-rectifying potassium channel SKOR. *FEBS Lett* 466:351–354.
60. Sentenac H, et al. (1992) Cloning and expression in yeast of a plant potassium ion transport system. *Science* 256:663–665.
61. Gaymard F, et al. (1996) The baculovirus/insect cell system as an alternative to *Xenopus* oocytes. First characterization of the AKT1 K^+ channel from *Arabidopsis thaliana*. *J Biol Chem* 271:22863–22870.
62. Lagarde D, et al. (1996) Tissue-specific expression of *Arabidopsis* AKT1 gene is consistent with a role in K^+ nutrition. *Plant J* 9:195–203.
63. Nieves-Cordones M, Alemán F, Martínez V, Rubio F (2014) K^+ uptake in plant roots. The systems involved, their regulation and parallels in other organisms. *J Plant Physiol* 171:688–695.
64. Kosegarten H, Grolig F, Esch A, Glüsenkamp K-H, Mengel K (1999) Effects of NH_4^+, NO_3^- and HCO_3^- on apoplast pH in the outer cortex of root zones of maize, as measured by the fluorescence ratio of fluorescein boronic acid. *Planta* 209:444–452.
65. Yu Q, Kuo J, Tang C (2001) Using confocal laser scanning microscopy to measure apoplastic pH change in roots of *Lupinus angustifolius* L. in response to high pH. *Ann Bot* 87:47–52.
66. Serowy S, et al. (2003) Structural proton diffusion along lipid bilayers. *Biophys J* 84: 1031–1037.
67. Fasano JM, et al. (2001) Changes in root cap pH are required for the gravity response of the *Arabidopsis* root. *Plant Cell* 13:907–921.
68. Poitout A, et al. (2017) Local signalling pathways regulate the *Arabidopsis* root developmental response to *Mesorhizobium loti* inoculation. *J Exp Bot* 68:1199–1211.
69. Schulte A, Lorenzen I, Böttcher M, Plieth C (2006) A novel fluorescent pH probe for expression in plants. *Plant Methods* 2:7.